JOURNAL OF CATALYSIS 53, 106–115 (1978)

Changes in the Surface and Catalytic Properties of Cane Sugar Carbons during Their Use as Catalysts in the Decomposition of 1,2-Dichloroethane

J. ZLOTNICK,[1] J. J. PRINSLOO, AND P. C. VAN BERGE

Department of Chemistry, Rand Afrikaans University, Johannesburg, South Africa

Received July 8, 1976; revised October 5, 1977

Activated cane sugar carbons with and without impregnated $BaCl_2$ have been used as catalysts in the vapor phase dehydrochlorination of 1,2-dichloroethane to vinyl chloride. Differences in BET areas determined with N_2 and 1,2-dichloroethane as adsorbates, the decrease in catalytic activity, changes in isotherm shape, and changes in surface texture of these catalysts during the course of this reaction have been recorded. These changes are interpreted in terms of the uniform crustation of a micropore and "ink-bottle" type of pore system, the nascence of new larger pores, and a pore-unblocking mechanism.

INTRODUCTION

It has been shown that the dehydrochlorination of 1,2-dichloroethane (DCE) on a carbon catalyst involves the decomposition of an adsorbed activated DCE complex into vinyl chloride (VC) and hydrochloric acid (*1*). However, the industrial application of this decomposition is hindered by a rapid decrease in catalytic activity. In the present work an attempt is made to follow through and interpret the deactivation and textural changes of activated cane sugar carbons, with and without impregnated $BaCl_2$, during the course of this heterogeneous reaction. Such textural changes have been deduced from the N_2 adsorption isotherms at $-195°C$ on the carbon catalysts taken out of the reactor at various stages during the course of the dehydrochlorination of DCE to VC.

[1] Present address: Witwatersrand College for Advanced Technical Education, Johannesburg, South Africa.

EXPERIMENTAL

The carbon catalysts were prepared by heating refined cane sugar carbons first at 400°C and then at 800°C in a closed muffle and pelleting the ground product with additives such as pure organic binders. The final pellets were fired at 500°C and granulated. The granules were activated at 950°C with CO_2 and air (*2*). The catalytic behavior of $BaCl_2$ and other metal chlorides is well recorded; a free radical mechanism involving $Cl^{\cdot}$ has been proposed (*3–5*).

The kinetic experiments were carried out with a continuous flow reactor coupled to a gas chromatograph as described in (*1*). The activity, determined as percentage conversion per gram of catalyst, was periodically recorded during the course of the reaction. Samples of the catalyst were periodically removed from the reactor. Adsorption isotherms for these catalyst samples were determined by a known volumetric method using pure N_2, at $-195°C$, as an adsorbate; this temperature

0021-9517/78/0531-0106$02.00/0

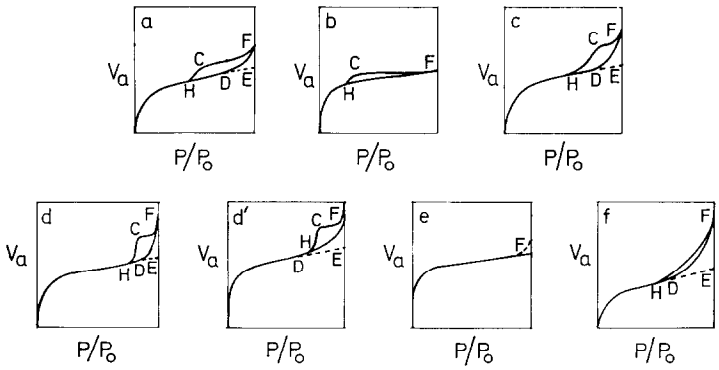

FIG. 1. A schematic classification of low temperature (−195°C) N_2 adsorption isotherms and hysteresis loops of impregnated and nonimpregnated activated cane sugar carbons.

was controlled by an auxiliary manometer (*2*, *6*). From these isotherms, BET areas as well as pore-size distribution (PSD) data in the pore radius range of 0 to 100 nm were obtained. The latter employed a method based on a cylindrical pore model (*7*). It was shown that for these carbons PSD results based on this model were comparable to those based on other models such as the "$V_a - t$" method (*2*). A blank experiment, without DCE, under the same experimental conditions was also done. BET areas were also determined with DCE as adsorbate at 15°C using a Perkin–Elmer Shell Model 212D sorptometer (*8*). The DCE was introduced into the sorptometer according to a method described by Schwab and Knözinger (*9*). Helium was used as a carrier gas. The partial pressure of the DCE was determined with the gas chromatograph. An estimated value of 2 nm^2 for the area of the adsorbed DCE molecule was used in the calculations.

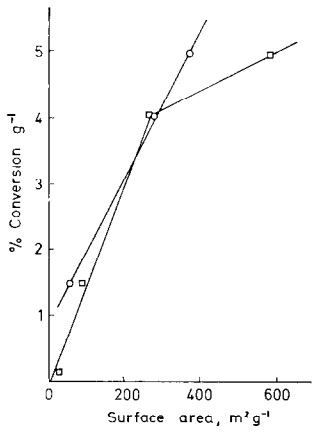

FIG. 2. Poisoning of catalyst 9 at 329°C. □, BET (N_2) area; and ○, BET (DCE) area.

Electron scanning microscopy, electron probe microscopy, and X-ray mapping of Ba^{2+} on the carbon surface was done. Helium densities were also determined for some of the carbons.

RESULTS

The only gases which could be detected under the prevailing experimental conditions were VC and hydrochloric acid and some acetylene at high conversions. The reactivity of all the catalysts decreased during the course of the reaction. An average increase in catalyst mass of 0.173 and 0.134 g per mol of VC for the nonimpregnated and impregnated carbons, respectively, was found. No changes in the isotherm, BET area, and PSD data of the carbon were detected as a result of the blank experiment.

A schematic classification of the isotherm types obtained is shown in Fig. 1. They consist of type I (BDDT) with varying amounts of type II or type IV character (*10*). Deactivation effects are illustrated in

Figs. 2–5. The data for the latter were obtained from the samples withdrawn at various times during the run by noting the percentage conversion at that time. Thereafter textural data as well as BET areas with N_2 and DCE as adsorbates were established. Variations of surface textural parameters with impregnation are shown in Table 1 and variations of these parameters with deactivation and time in the reactor, in columns 1–12 of Tables 2 and 3 and columns 4–7 of Table 4. The latter table also includes the comparison of BET areas determined with N_2 and DCE. Other deactivation data are shown in columns 13–16 of Tables 2 and 3.

The headings to Tables 1–3 are explained below.

Columns 3–6: PSD data. A represents the fraction of the BET area of all the pores in a given pore radius range in nanometers written as a subscript to A. A micropore is here defined as an ideal cylinder with a radius less than 1 nm.

Column 7: The total pore volume.

Column 8: The P/P_0 coordinate of the point D in Fig. 1 where the isotherm commences to rise steeply toward the $P/P_0 = 1$ axis.

Column 9: The P/P_0 coordinate of the point H in Fig. 1 where the hysteresis loop closes.

Column 10: The area of the hysteresis loop. This quantity has been proposed as a semiquantitative measure of the extent of change in pore shape as well as the contribution to hysteresis by a given pore type (*2*).

Column 11: The mean pore radius, $\bar{r}$, of a cylindrical pore as given by $2\ V_p/(\text{BET area})$.

Column 14: The partial pressure of VC, conveniently expressed in millimeters of mercury (1 mm Hg = 133.3 Pa).

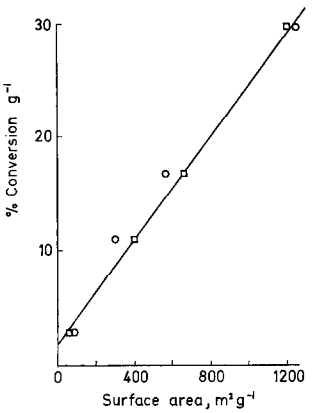

FIG. 4. Poisoning of catalyst 11 at 388°C. □, BET (N_2) area; and ○, BET (DCE) area.

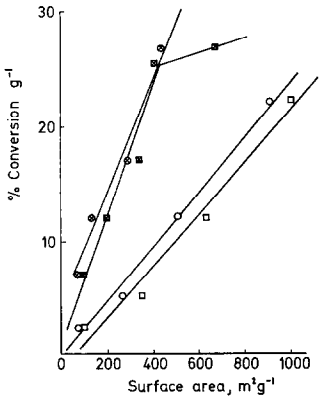

FIG. 3. Poisoning of catalysts at 400°C. □, BET (N_2) area; and ○, BET (DCE) area of catalyst 11. ⊠, BET (N_2) area; and ⊗, BET (DCE) area of catalyst 12.

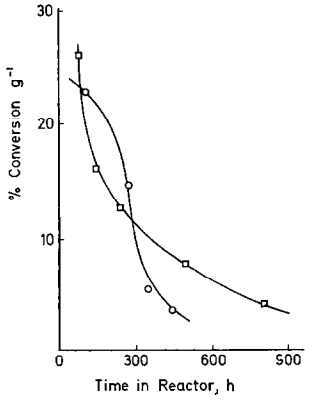

FIG. 5. Degree of poisoning of catalysts at 400°C with time in the reactor and partial pressure of DCE = 1.649×10^4 Pa. □, catalyst 12; and ○, catalyst 11.

TABLE 1

Pore-Size Distribution and N_2 (−195°C) Adsorption Isotherm Data Showing the Effect of Impregnation with ca. 30% $BaCl_2$ on Activated Cane Sugar Carbons, U. S. Standard Mesh 20–35

1. Carbon reference no.	2. BET (N_2) area ($m^2\ g^{-1}$)	3. A_{0-1}	4. A_{1-2}	5. A_{2-10}	6. A_{10-100}	7. V_p ($cm^3\ g^{-1}$)	8. xD	9. xH	10. AH [cm^3 of N_2 (STP) g^{-1}]	11. $\bar{r}$ (nm)	12. Isotherm type (see Fig. 1)
1[a]	1340	0.870	0.100	0.028	0.002	0.600	0.77	0.69	0.50	0.90	a
2[b]	839	—	—	—	—	0.379	0.74	0.75	0.28	0.90	a
3[c]	867	—	—	—	—	0.391	0.68	0.70	0.35	0.90	a
4[a]	122	0.812	0.131	0.055	0.002	0.061	—	—	—	1.00	c
5[b]	124	0.823	0.121	0.056	0.002	0.066	—	—	—	1.06	c
6[c]	164	0.890	0.067	0.041	0.002	0.077	0.97	—	—	0.94	c
7[a]	835	0.880	0.090	0.029	0.001	0.360	0.64	0.64	0.94	0.86	c
8[b]	477	0.849	0.101	0.048	0.002	0.223	0.92	—	—	0.94	c
9[a]	992	0.890	0.080	0.028	0.002	0.440	0.91	0.64	0.50	0.89	a
10[b]	596	0.879	0.081	0.039	0.002	0.268	0.88	—	—	0.89	c
11[d]	1118	0.491	0.445	0.061	0.003	0.670	0.87	0.84	0.76	1.20	c
12[b]	665	0.587	0.356	0.053	0.005	0.372	0.85	0.81	0.38	1.12	c

[a] Nonimpregnated carbons with a high initial micropore content.
[b] Impregnated with ca. 30% $BaCl_2$ of carbon mass.
[c] Isotherms determined on selected black granules of the impregnated carbons.
[d] Nonimpregnated carbons with a low initial micropore content.

Column 15: The estimated pore area accessible to the DCE molecule calculated from $(A_{0-1})/2 + A_{1-100}$. The estimate was based on extrapolated data for similar compounds (*11*, *12*).

Column 16: The decrease in the pore area accessible to the DCE molecule, D(EAA), divided by the number of moles of VC produced, MVC.

Column 17: Helium (absolute) densities of the carbons.

Percentage $\Delta V_p/V_p$ is the difference between the liquid adsorbate uptake at F in Fig. 1 and the pore volume, divided by the pore volume, expressed as a percentage. Its magnitude indicates the presence of large pores between xD and $P/P_0 = 1$. The average flow rates, the temperature of the reaction, and the partial pressure of the DCE (expressed in pascals), all of which are constant for a given run, are shown as footnotes to Tables 2 and 3. The meaning of the headings to Table 4 follows from the above.

Electron microscopy on the impregnated carbons showed partial covering up of the original pore mouths of the larger pores, the deposition of fine $BaCl_2$ crystal debris up to 100 nm in "width," and the exposure of underlying carbon through breaks in the $BaCl_2$ film. However, the presence of actual deposits inside the fine pores was not discernable. A redistribution of $BaCl_2$ over the carbon surface after use in the reactor was also observed by X-ray mapping of Ba^{2+} (*13*).

Helium densities done on the two nonimpregnated carbons decreased with decrease in BET area. Comparisons could not be done for the impregnated carbons because of the uneven deposition of $BaCl_2$ over the surface of the carbon granules.

DISCUSSION

The observed increase in catalyst mass during the reaction can be explained by carbon deposition. This has been previously reported and interpreted via several possible side paths (*3*, *4*, *14–16*). The results of the blank experiment ruled out the possibility of pore blocking by mass transfer along the carbon surface as a complementary side effect.

An upswing of the isotherm near the saturation axis of $xD > 0.95$, say, for BDDT types I and IV isotherms, represents

TABLE 2

Pore-Size Distribution, Reactor Conditions, and N_2 (−195°C) Adsorption Isotherm Data of Activated Cane Sugar Carbons, U. S. Standard Mesh 20–35, during Their Use as Catalysts in the Dehydrochlorination of DCE

1. Carbon reference no.	2. BET (N_2) area ($m^2\ g^{-1}$)	3. A_{0-1}	4. A_{1-2}	5. A_{2-10}	6. A_{10-100}	7. V_p ($cm^3\ g^{-1}$)	8. xD	9. xH	10. AH [cm^3 of N_2 (STP) g^{-1}]	11. $\bar{r}$ (nm)	12. Isotherm type (see Fig. 1)	13. Time in reactor (hr)	14. P_{VC} (mm Hg)	15. EAA ($m^2\ g^{-1}$)	16. $\frac{D(EAA)\times10^{-3}}{MVC}$ ($m^2\ g^{-1}\ mol^{-1}$)	17. ρHe ($g\ cm^{-3}$)
9[a]	992	0.890	0.080	0.028	0.002	0.440	0.91	0.64	0.50	0.89	a	0	19.4	551	—	1.79
	582	0.859	0.110	0.027	0.004	0.263	0.83	0.83	0.15	0.91	c	29.0	19.4	332	2.47	—
	477	0.811	0.130	0.058	0.004	0.232	0.82	0.82	0.10	0.97	c	37.0	19.9	283	1.95	—
	267	0.610	0.307	0.075	0.006	0.157	0.82	0.82	0.20	1.18	c	56.0	15.8	186	1.82	—
	267	0.610	0.307	0.750	0.006	0.157	0.82	0.82	0.20	1.18	c	56.0[b]	108.9	186	1.82	—
	85	0.435	0.365	0.188	0.012	0.064	0.89	0.86	0.15	1.50	d	68.0	41.5	57	1.00	1.21
	24	0.375	—	—	—	0.039	0.92	0.92	0.15	3.28	d	150.0	4.1	19	0.15	—
11[c]	1118	0.491	0.445	0.061	0.003	0.670	0.87	0.84	0.76	1.20	c	0	42[d]	843	—	—
	1060	0.523	0.358	0.113	0.005	0.695	0.90	0.87	0.70	1.31	c	95.0	42.1	782	0.09	—
	678	0.375	0.534	0.084	0.007	0.452	0.87	0.84	0.45	1.33	c	265.0	24.4	551	0.26	—
	361	0.396	0.479	0.119	0.007	0.348	0.88	0.83	0.30	1.38	c	337.0	9.4	300	1.29	—
	72	0.153	0.583	0.139	0.125	0.073[e]	0.79	0.71	2.50	2.03	f	373.0	5.4	66	5.57	1.32

[a] Carbons with a high initial micropore content. Reactor temperature, 329°C; partial pressure of DCE, 2.48×10^4 Pa; average flow rate, 5920 $cm^3\ hr^{-1}$; initial mass of carbon, 1.50 g.
[b] Temperature increased instantaneously to 406°C.
[c] Carbons with a low initial micropore content. Reactor temperature, 400°C; partial pressure of DCE, 1.65×10^4 Pa; average flow rate, 6700 $cm^3\ hr^{-1}$; initial mass of carbon, 1.50 g.
[d] Approximate value.
[e] V_a difficult to establish accurately on the steep slope near $P/P_0 = 1$ axis.

TABLE 3

Pore-Size Distribution, Reactor Conditions, and N_2 (−195°C) Adsorption Isotherm Data of Activated Cane Sugar Carbons, Impregnated with ca. 30% $BaCl_2$, U. S. Standard Mesh 20–35, during Their Use as Catalysts in the Dehydrochlorination of DCE

1. Carbon reference no.	2. BET (N_2) area ($m^2\ g^{-1}$)	3. A_{0-1}	4. A_{1-2}	5. A_{2-10}	6. A_{10-100}	7. V_p ($cm^3\ g^{-1}$)	8. xD	9. xH	10. AH [cm^3 of N_2 (STP) g^{-1}]	11. $\bar{r}$ (nm)	12. Isotherm type (see Fig. 1)	13. Time in reactor (hr)	14. P_{VC} (mm Hg)	15. EAA ($m^2\ g^{-1}$)	16. $\frac{D(EAA)\times10^{-3}}{MVC}$ ($m^2\ g^{-1}\ mol^{-1}$)
10[a]	596	0.879	0.081	0.039	0.002	0.268	0.88	—	—	0.89	e	0	147.5	334	—
	501	0.830	0.130	0.038	0.003	0.237	0.81	0.74	0.42	0.94	c	27.0	66.5	293	0.11
	81	0.531	0.284	0.173	0.012	0.061	0.82	0.82	0.10	1.43	e	46.0	32.8	60	1.76
	28	0.393	—	—	—	0.038	0.83	0.83	0.15	2.70	d	75.0	20.1	22	0.36
	22	0.364	—	—	—	0.033	0.88	0.80	0.25	2.90	d	93.0	15.2	18	0.09
	<20	—	—	—	—	<0.03	—	—	—	ca.3	—	175.0	15.2	<18	<0.09
12[b]	665	0.587	0.356	0.053	0.005	0.372	0.85	0.81	0.38	1.12	c	0	50.0	470	—
	420	0.145	0.736	0.107	0.012	0.318	0.85	0.82	0.36	1.51	c	74.0	48.2 30.3	358	0.19
	335	0.382	0.531	0.081	0.005	0.220	0.90	0.87	0.37	1.24	c	142.5	32.2 34.2	271	0.26
	213	0.347	0.545	0.099	0.009	0.156	0.80	0.81	0.35	1.46	d	239.15	20.8 16.3	176	0.22
	93	0.097	0.742	0.140	0.022	0.080	0.82	0.84	0.17	1.72	d′	481.3	10.5 7.5	88	0.17
	58	0.535	0.293	0.155	0.017	0.047	0.62	0.88	0.10	1.62	d′	792.0	4.8	43	0.15

[a] Carbons with a high initial micropore content impregnated with 30% $BaCl_2$. Reactor temperature, 407°C; partial pressure of DCE, 2.48×10^4 Pa; average flow rate, 5920 $cm^3\ hr^{-1}$; initial carbon mass, 1.50 g.

[b] Carbons with a low initial micropore content impregnated with 30% $BaCl_2$. Reactor temperature, 400°C; partial pressure of DCE, 1.65×10^4 Pa; average flow rate, 6799 $cm^3\ hr^{-1}$; initial carbon mass, 1.50 g.

TABLE 4

Comparative Reactor Conditions, Pore-Size Distribution, and BET Area Data of Impregnated and Nonimpregnated Activated Cane Sugar Carbons, U. S. Standard Mesh 20–35, during Their Use as Catalysts in the Dehydrochlorination of DCE

1. Carbon reference no.	2. Time in reactor (hr)	3. Reaction temperature (°C)	4. BET (N_2) area ($m^2\ g^{-1}$)	5. BET ($C_2H_4Cl_2$) area ($m^2\ g^{-1}$)	6. A_{0-1}	7. A_{1-100}
9	0	—	992	410	0.89	0.11
	56	329	297	279	0.61	0.39
12	0	—	665	362	0.59	0.41
	143	400	335	284	0.38	0.62
11	0	—	1118	702	0.49	0.51
	30	388	1209	1257	0.28	0.72
11	0	—	1118	702	0.49	0.51
	265	400	678	498	0.38	0.62

liquid adsorbate uptake in macropores or in large interparticle spaces. These experimental isotherms can be considered as the superimposition of several isotherm types related to various pore shapes. The contribution of types I and IV (or II) toward the upswing could be significant particularly for the case of large xD values (e.g., $xD > 0.85$) as is the case for most of the carbons. Changes in xD values are therefore significant in the detection of the presence of large pores.

The xH values were used to indicate the appearance of hysteresis in pores of a given size. Tensile effects were ignored since the same type of adsorbent, at the same temperature, with the same adsorbate was used throughout for $xH > 0.5$. Generally changes in xD and xH values, as will be discussed below, were considered as supplementary to the PSD data.

(a) *The Effect of Impregnation with $BaCl_2$ (Refer to Table 1)*

Those carbons with a low initial BET area showed little change in BET area and pore volume while those with a high initial BET area showed a decrease of up to 50%. All the carbons showed little change or some increase in xD, an increase or elimination of xH, a decrease or elimination of AH, and little change in percentage $\Delta V_p/V_p$ values. This points to preferential blocking of the smaller pores as well as the blocking and/or change in shape of hysteresis-producing pores to nonhysteresis-producing pores for the case of the larger pores.

For certain carbons which were not used for kinetic purposes, $BaCl_2$ deposition was nonuniform and some granules were free of white $BaCl_2$ patches. These selected granules showed higher AH, BET area, and pore volume as well as somewhat lower xD and xH values than the impregnated mixed batch samples or even the original samples for the case of the carbons with a low initial BET area. This points to granule disintegration and/or the unblocking of debris-clogged pore mouths. The decrease of the A_{0-1}/(BET area) ratio points to the blocking of micropores while the increase in this ratio for carbons with a low initial micropore content shows an unblocking of pores. The blocking exerts a greater influence on the carbons with a high initial BET area and the unblocking on carbons with a low initial BET area. The unblocking could also account for the absence of a significant decrease in $\bar{r}$

values. Electron microscopy does not contradict these conclusions.

(*b*) *The Effect of the Dehydrochlorination of 1,2-Dichloroethane (DCE) (Refer to Tables 2–4 and Figs. 2–5)*

The following is evident from the tables:

(*i*) *Changes in surface area and pore volume.* For both the impregnated as well as the nonimpregnated carbons, the cumulative crustation effect of carbon deposition reduced BET areas and pore volumes to below 30 m^2g^{-1} and 0.03 cm^3 g^{-1}, respectively. For the carbons with a high initial micropore content, changes in pore-size distribution resulted in A_{1-100} maintaining a narrow range between 50 and 95 m^2 g^{-1} down to a BET area of ca. 250 m^2 g^{-1}. For the carbons with a lower initial micropore content the A_{1-100} values covered a wider range. Pore volume changes were similar to those of area, while the mean pore radius increased with a decrease in BET area. These results may be interpreted as follows:

The presence of "ink bottles" in these carbons has been established (*2*). Minimal crustation causing but thin-layer deposition in these pores would block the narrow pore entrances, sealing off the pore areas and volumes. This would result in a decrease in A_{0-1}/(BET area), an increase in $\bar{r}$, and very large initial decreases in BET area and pore volume. The decrease in helium density confirms this possibility. This effect would be less pronounced for the carbons with a low initial micropore content and is also countered by the unblocking effect. This is confirmed by the small decrease and even increase in BET area after short sojourn in the reactor (e.g., from 1118 to 1209 m^2 g^{-1} after 30 hr). Subsequent regular decreases in area and pore volume resulted from the cumulative uniform deposition on the walls of the larger pores. The exponential increase in $\bar{r}$ and percentage $\Delta V_p/V_p$ (e.g., 3.4 to 31 for the carbons with a high initial micropore content) points to even larger pores at high crustation and low BET area.

(*ii*) *Changes in xD and xH values.* For all the carbons which initially had a high xD value this parameter remained comparatively constant except for some increase at low BET areas. This confirms the maintenance of large pores and the subsequent appearance of even larger pores. Carbons with a low initial micropore content showed some decrease in xD after long sojourn in the reactor. This may be due to some unblocking of smaller pores and/or crustation narrowing of larger pores over and above pore-shape changes. Carbons with a high initial BET area, a high initial micropore content, and a small initial xD value showed an increase in this parameter (e.g., from 0.67 to 0.80 after 48 hr; not shown in tables). This is in keeping with crustation blocking of smaller pores. The nascence of an xD value for a carbon with a low initial BET area and a high initial micropore content points to unblocking or creation of larger pores (e.g., from 0 to 0.96 after 48 hr; not shown in tables).

For all the carbons, large xH values were maintained while smaller values were increased to a maximum at low BET area. Thus crustation eliminated hysteresis from smaller pores only. xH eliminated by impregnation reappeared during the reaction. This points to the unblocking of $BaCl_2$ from hysteresis-producing pores. After long sojourn in the reactor some decrease in xH was observed for the carbons with a low initial micropore content. This could be due to either the unblocking of smaller hysteresis-producing pores and/or the crustation narrowing of larger nonhysteresis pores to hysteresis-producing pores.

(*iii*) *Changes in hysteresis loop shape.* Loop shapes changed from types a to c to d (Fig. 1) with further changes to f and d′

for impregnated carbons. Types d and d' resemble pore shape XV of a known classification (*17*) usually consisting of interparticle spaces built up from spherical particles. Type f is compatible with shape XV, superimposed by other types including nonhysteresis-producing pores which thinned the loop. *AH* values after progressively diminishing with crustation increased again at low BET areas. This too supports the possible naissance of a system of larger hysteresis-producing pores. Electron microscopy observations also confirm this. These pore spaces could result from a coral-type crustation buildup which could entail the transformation of hysteresis-producing to nonhysteresis-producing pores and vice versa.

(*iv*) *Changes in catalyst activity.* The observed decrease in catalyst activity (Figs. 2–5) accompanied the decrease in surface area and concurs with the mechanism of a DCE complex on the catalyst surface (*1*). The decrease in activity, however, was not always proportional to the decrease in the surface area as determined with N_2. From Figs. 2 and 3 it can be seen that for catalysts 9 and 12 the activity initially decreased less than could be expected from the decrease in surface area. This is consistent with the initial blocking of the micropores which make a minor contribution area-wise to the activity. The catalytic effect of $BaCl_2$ countered the lower initial micropore content of catalyst 11. This can be caused either by a diffusion limitation of the reaction in these spaces or by an inaccessibility of the micropores to the DCE molecules. Calculations have shown that the reaction in the micropores is not diffusion-controlled under the prevailing experimental conditions (*18*).

The alternative possibility that the DCE molecule is too large to enter the micropores is therefore more probable and is further substantiated by the following: Plots of activity against BET area as determined with DCE were linear. Also large differences in the values in columns 4 and 5 of Table 4 for the high micropore ratio catalysts were noted.

It was observed that for the case of the nonimpregnated catalyst 11 there was a proportionality between BET (N_2) areas and catalytic activity. This apparent contradiction can be explained by the much smaller micropore ratio of this carbon.

Supplementary to the accessibility factor of the DCE molecule discussed above, useful conclusions on the change in catalyst activity can also be drawn from the parameter D(EAA)/MVC. For the carbons with a high initial micropore content, the value of D(EAA)/MVC decreased with time. This correlates with the previous suggestion that an initial sealing off of large EAA occurs. This parameter decreases gradually with time because the proportion of micropores decreases, and at low BET areas there appears to be the nascence of new larger pores.

For the carbons with a low initial micropore content at 400°C, the initial value of D(EAA)/MVC was lower than for the carbons with a high initial micropore content and thereafter increased with time. In other experiments at lower temperatures (379 and 338°C) the same carbon as that in Table 2 showed a low or even a negative initial D(EAA)/MVC value which thereafter decreased and then increased somewhat after a long sojourn (823 hr) in the reactor. The low initial D(EAA)/MVC values agree with the lower narrow neck pore content, while the negative values would be in accordance with the unblocking effect. At the highest temperature the gradual increase in D(EAA)/MVC with time may be due to the greater contribution of the carbon deposition side reaction. For this reason the experiments at the lower temperatures first showed some decrease since the influence of the side reaction shows itself after a longer period in the reaction.

For the impregnated carbons with a high

as well as with a low initial micropore content, the D(EAA)/MVC values increased at the beginning and thereafter decreased. This decrease after a long sojourn in the reactor is due to the smaller contribution of the side reaction as a result of the greater activity of $BaCl_2$ at the smaller areas.

REFERENCES

1. Prinsloo, J. J., van Berge, P. C., and Zlotnick, J., *J. Catal.* **32**, 466 (1974).
2. Zlotnick, J., van Berge, P. C., and Prinsloo, J. J., *J. S. Afr. Chem. Inst.* **27**, 70 (1974).
3. Barton, D. H., and Howlett, K. C., *J. Chem. Soc.*, 155 (1949).
4. Ghosh, J. C., and Rama, S., *Petroleum* **14**, 261 (1951).
5. Medonos, V., Ruzicka, V., and Silinek, K., *Chem. Prumysl.* **11**, 229 (1961).
6. Lippens, B. C., Linsen, B. G., and De Boer, J. H., *J. Catal.* **3**, 32 (1964).
7. Clement, C., Montarnal, R., and Trambouze, P., *Rev. Inst. Fr. Petrole Ann. Combust. Liquides* **17**, 558 (1962).
8. Nelsen, F. M., and Eggertsen, F. T., *Anal. Chem.* **30**, 1387 (1958).
9. Schwab, G. M., and Knözinger, H., *Z. Physik. Chem.* **37**, 230 (1963).
10. Brunauer, S., Deming, L. S., Deming, W. S., and Teller, E., *J. Amer. Chem. Soc.* **62**, 1723 (1940).
11. Gregg, S. J., and Sing, K. S. W., "Adsorption, Surface Area, and Porosity," pp. 75–80. Academic Press, New York, 1967.
12. Mclellan, A. L., and Harnsberger, H. F., *J. Colloid Interface Sci.* **23**, 577 (1967).
13. Zlotnick, J., Ph.D. thesis. Rand Afrikaans University, Johannesburg, 1975.
14. Doraiswamy, L. K., Brahme, P. H., Pai, M. U., and Chidambaram, S., *Brit. Chem. Eng.* **5**, 618 (1960).
15. Chervinskii, K. A., Sukhopar, P. A., and Zakharov, I. N., *Khim. Prom.* 1, 21 (1961).
16. Paushkin, Ya. M., and Charnaya, E. G., *Sov. Chem. Ind.* **4**, 294 (1971).
17. De Boer, J. H., *in* "The Structure and Properties of Porous Materials" (D. H. Everett and F. S. Stone, Eds.), pp. 68–94. Butterworths, London, 1958.
18. Prinsloo, J. J., Ph.D. thesis. Rand Afrikaans University, Johannesburg, 1975.